Analysis of the Isothermal Crystallization of Isotactic Polypropylene Nucleated with Sorbitol Derivatives

C. Marco,[1] G. Ellis,[1] M. A. Gómez,[1] J. M. Arribas[2]

[1]*Departamento de Física e Ingenieria, Instituto de Ciencia y Tecnología de Polímeros, CSIC, c/ Juan de la Cierva 3, 28006 Madrid, Spain*
[2]*Dirección Corporativa de Servicios Compartidos, Centro de Tecnología REPSOL-YPF, Ctra. Extremadura N-V, km. 18, Desvío Villaviciosa de Odón, 28931 Móstoles (Madrid), Spain*

Received 28 January 2002; accepted 12 August 2002

ABSTRACT: The isothermal crystallization kinetics of isotactic polypropylene (iPP) and iPP nucleated with the sorbitol derivatives 1,3:2,4-bis(4-methyldibenzylidene)sorbitol and 1,3:2,4-bis(3,4-dimethylbenzylidene)sorbitol was studied, along with the subsequent melting behavior, as a function of the nucleating agent concentration. The influence of the agents on the crystallization rate, crystallization temperature, and crystallization range was examined. The isothermal crystallization temperature increased, along with the crystallization rate, with increasing nucleating agent concentration. The maximum effect of the additives occurred at concentrations of 0.3% or greater. © 2003 Wiley Periodicals, Inc. J Appl Polym Sci 88: 2261–2274, 2003

Key words: isotactic; poly(propylene) (PP); nucleation; crystallization

INTRODUCTION

The crystallization of polymeric materials is generally described in terms of a crystalline nucleation and growth model,[1] where it is assumed that nuclei form from ordered material as a result of thermal fluctuations in the melt. These nuclei then grow by the addition of more material until a stable crystalline structure develops. Thus, the course of crystallization is determined by both the rate of nucleation and the rate of crystalline growth, showing an extraordinary dependence on the undercooling and, consequently, on the temperature of crystallization. The processes of nucleation and growth have been extensively studied in both monomeric and polymeric systems. In the latter case, two main schools have developed: one provides information on the crystallization behavior and the crystalline morphology with thermodynamic approximations,[2] and the other offers a description of the kinetics of formation and growth of the crystalline nuclei.[3,4]

The crystallization of polymers can be analyzed by the observation of the growth of a specific crystal face, the growth rate of a crystalline superstructure, or the overall rate of crystallization and is the result of the rate of formation and growth of a stable nucleus and the rate at which the polymer chains are incorporated to the growing crystalline faces. In these materials, the rate of formation of a stable nucleus not only depends on the crystallization temperature (T_c), that is, the undercooling of the system, but it is also a function of the energetic contribution necessary for the formation of the nucleus, or the free energy of nucleation, and the energetic contribution associated with the transport of the polymeric chains over the melt–crystal interface. At low undercooling, that is, at temperatures relatively close to the melting temperature (T_m), and as such, in isothermal experimental conditions, the rate of formation of crystalline nuclei is minimal, the crystallization process is controlled by the nucleation stage, and the rate of the process shows a strongly negative coefficient with the T_c. However, in regions where the T_c is low, that is, at high undercooling, and in the majority of cases distant from isothermal conditions, the transport of the polymeric chains at the crystal-melt interface becomes more difficult as it approaches the glass-transition region and, thus, controls the crystallization rate with a positive temperature coefficient. The balance between both processes, nucleation and transport, generates a maximum in the crystallization rate, with antagonistic temperature coefficients, which makes the selection of the interval of T_c's in polymeric materials extremely important.

The use of nucleating agents (NAs) in isotactic polypropylene (iPP) is widespread and of great commercial importance because the control of the crystallization process allows one to modify the optical, me-

Correspondence to: C. Marco (cmarco@ictp.csic.es).
Contract grant sponsor: Comisión Interministerial de Ciencia y Tecnología; contract grant number: MAT98-0914.
Contract grant sponsor: Comunidad Autónoma de Madrid; contract grant number: 07N/0032/1999.

Journal of Applied Polymer Science, Vol. 88, 2261–2274 (2003)

chanical, and surface properties of a given system to suit the particular application by the adjustment of the type and dispersion of the agent in the polymer. A large number of substances that nucleate the monoclinic crystalline modification of iPP have been described. Sorbitol derivates are among the most efficient[5–9] and have been used extensively during the last decade to improve the transparency of iPP. The first-generation NAs based on sorbitol derivatives include the widely used 1,3:2,4-bis(dibenzylidene)sorbitol (DBS) and 1,3:2,4-bis(*p*-methoxybenzylidene)sorbitol. Unlike organic salts, sorbitol-based NAs dissolve in the molten polymer, which gives rise to a homogeneous solution. As the polymer is cooled, the solution forms a finely meshed gel-like network of twisted DBS fibers, which, it is suggested,[5,10,11] promotes polymer crystallization via epitaxy. Although the mechanisms by which these agents act are still not clearly understood, a number of authors have related nucleating ability to geometrical and dimensional similarities between the additive and the growing crystalline lattice,[5,10,11] which can, in turn, condition the type of interactions between the additive and the polymer chain.[11–14] Subsequently, a series of modifications in the chemical structure have led to a second generation of sorbitol-based NAs comprised of halo and alkyl derivatives, such as 1,3:2,4-bis(*p*-methylbenzylidene)-sorbitol, 1,3:2,4(*p*-ethylbenzylidene)sorbitol, and 1,3:2,4-bis(*p*-chloro-*p*′-methylbenzylidene)sorbitol.[9] More recently, for high-temperature processing, the compound 1,3:2,4-bis(3,4-dimethylbenzylidene)sorbitol has been described[11,15] and represents the third generation and most modern example of sorbitol-based NAs for iPP. With this NA, we demonstrated[16] that during dynamic crystallization, nucleation efficiencies of 60–65% can be achieved, along with a large increase in the T_c's, even for the lowest additive concentration of 0.025%.

The aim of this study was to analyze the crystallization kinetics of iPP under isothermal conditions in the presence of sorbitol-based NAs and to study the subsequent melting behavior as a function of the nature and concentration of NA.

EXPERIMENTAL

Materials and preparation

The iPP sample was a commercial grade supplied by REPSOL-YPF (Madrid, Spain) with a viscosity average molecular weight (M_v) of 164,700 and a 95% isotacticity determined by solution NMR spectroscopy. The NAs were 1,3:2,4-*bis*-(4-methyldibenzylidene)sorbitol (Geniset MDG001, NJC-Rika, Osaka, Japan) and 1,3:2,4-*bis*-(3,4-dimethylbenzylidene) sorbitol (Millad 3988, Milliken Chemical, Gent, Belgium). The nucleated systems were prepared by melt blending in a twin-screw extruder with concentrations of NA between 0.025 and 1.0 wt% with conditions previously described.[16,17]

Differential scanning calorimetry (DSC)

Isothermal crystallization was undertaken in a Perkin Elmer DSC7/UNIX/7DX system, calibrated with indium (T_m = 156°C, melting enthalpy (ΔH_m) = 28.45 Jg^{-1}.).

We achieved reproducible crystallization isotherms with an initial thermal history cycle, melting the material at 210°C for 10 min and subsequently cooling at 64°C min^{-1} to the predetermined T_c, recording the exotherm as a function of time until the isothermal crystallization was considered to be complete, when the variation in the calorimetric baseline was less than 10^{-2} mW. The sample was then heated at 10°C min^{-1} to the T_m.

The degree or extent of crystalline transformation (θ) is obtained by partial integration from the following expression:

$$\theta = \frac{\int_0^t (dH/dt)\, dt}{\int_0^\infty (dH/dt)\, dt} \qquad (1)$$

where the first integral is the heat of crystallization generated in time t and the second integral is the total heat of crystallization for $t = \infty$, which allows the quantitative evolution of the crystallization process to be followed as a function of time.

RESULTS AND DISCUSSION

Isothermal crystallization kinetics

In homogeneous nucleation, the stable crystalline nuclei are generated from the existence of statistical fluctuations in the melt phase, and the rate of nucleation is constant. In the case of heterogeneous nucleation, the nucleation rate is not constant due to the presence of heterogeneities in the system with probabilities to induce or develop crystallinity. The nuclei present in the system at the start of crystallization include both heterogeneous and homogeneous or athermal nuclei. Heterogeneous nuclei are formed by particles that chemically differ from the crystallizable polymer, such as catalyzers, pigments, impurities, or NAs.

Because the rate of crystallization depends on the thermal history, memory effects are often observed in the slow crystallization of polymeric materials. However, the role of the heterogeneous nuclei can be regarded as surface defects whose sensitivity to the ther-

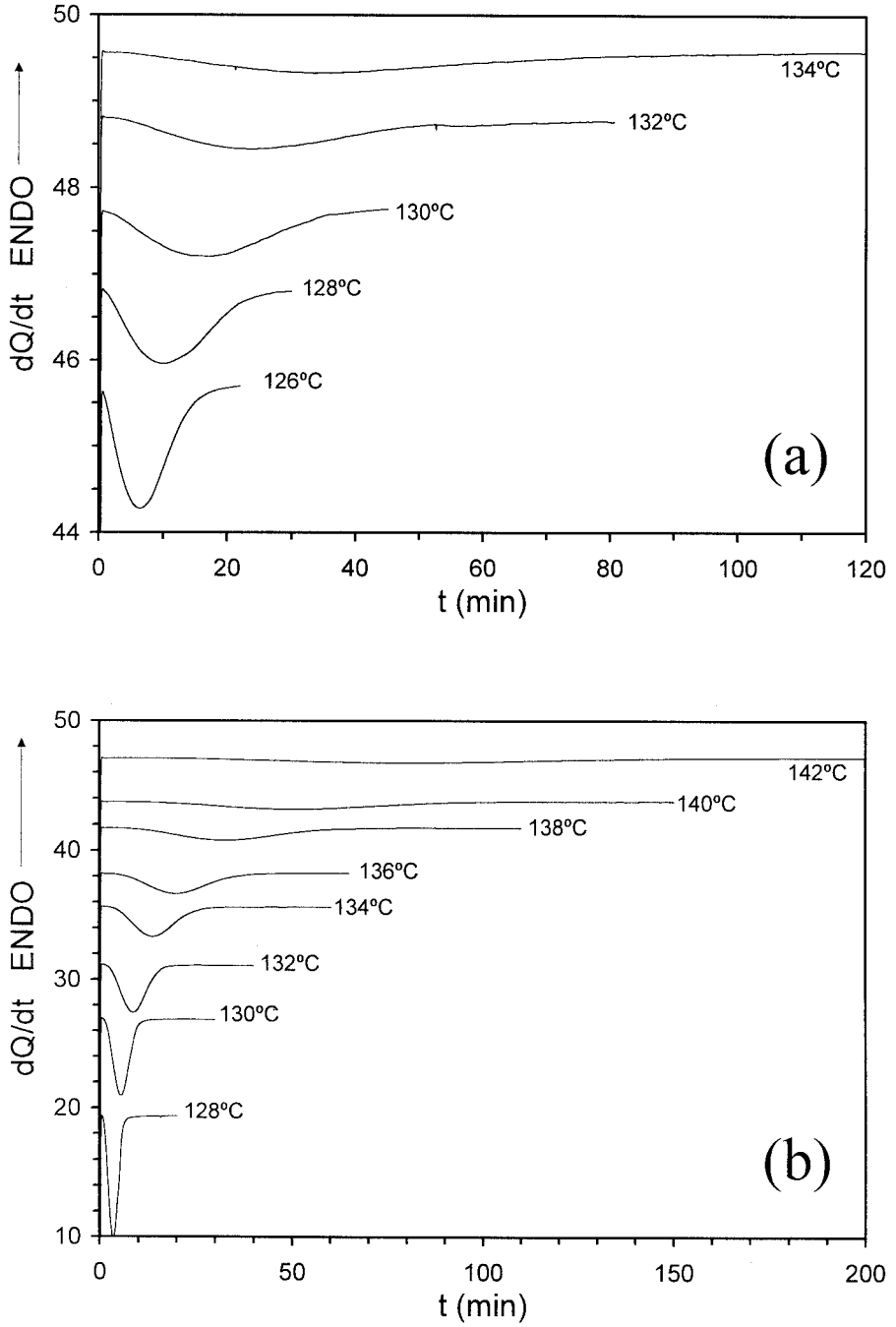

Figure 1 Crystallization exotherms under isothermal conditions at the temperatures indicated for (a) iPP and (b) iPP/Millad 3988 (0.05%).

mal history of the melt can be considered as very slight or almost inappreciable. However, the concentration of athermal nuclei, that is, preexisting crystalline domains in the melt with the same chemical structure as the molten polymer, is extraordinarily sensitive to the melt temperature and the residence time in the molten phase. In this regard, Ziabicki and Alfonso[18,19] developed a theoretical model that predicts memory effects related with the distribution of domain sizes, which control the concentration of predetermined crystalline nuclei and the initial rate of nucleation in the subsequent isothermal crystallization.

From previous studies that were carried out to eliminate melt-memory effects in nucleated iPP systems,[17] the thermal history selected for the analysis of the crystallization kinetics of iPP and the iPP/NA systems was 210°C and 10 min the melt temperature and residence time, respectively, after heating at 200°C min^{-1}. The crystallization exotherms are shown in Figure 1(a) where one can see that both the induction

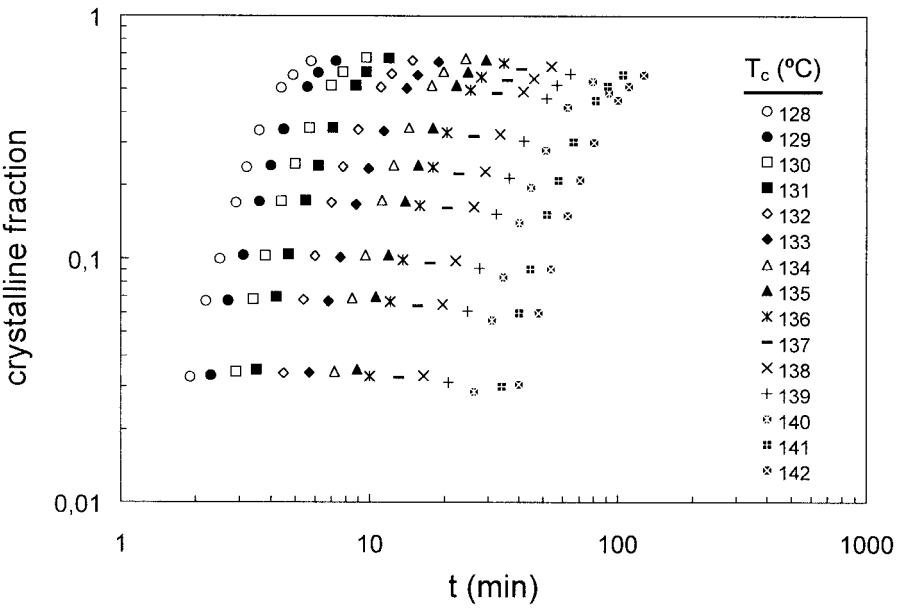

Figure 2 Göler-Sachs representation for the iPP/Millad 3988 (0.05%) system at the T_c's indicated.

period and the width of the exotherm increased progressively with increasing T_c, which clearly indicates a reduction in the crystallization rate as the undercooling, $\Delta T = T_m - T_c$ diminished. The reduction of the induction period as the undercooling increased resulted from the reduction in the critical size of the nuclei at lower T_c's.

In the analysis of the evolution of the isothermal crystallization exotherms of a sample of nucleated iPP, such as the example given in Figure 1(b), a behavior similar to that for pure iPP shown in Figure 1(a) is observed, with a progressive displacement in the temperature axis as the undercooling decreased. However, the most relevant difference was the increase in the temperature range in which crystallization took place in the presence of NAs over similar timescales. Thus, although in the case of pure iPP, the interval was between 127 and 134°C, in the case of iPP/NA this interval, considered globally for all the NAs and all compositions, was between 126 and 150°C, which appears to indicate an increase in the crystallization rate.

The development of crystallinity with time, that is, the phase change kinetics, was followed with the free growth approximation described by Göler and Sachs,[20] where it is assumed that the evolution of a crystalline nucleus and its subsequent growth is independent of the growth of other nuclei and of the already transformed material. In this case, the kinetic process of the transformation is described by

$$\ln(1 - \lambda)_t = -kt^n \qquad (2)$$

where $(1 - \lambda)_t$ is the amount of crystallinity developed in time t, k is a constant, and the exponent n defines the growth geometry, adopting values of 2, 3, or 4 for one-, two-, and three-dimensional growth, respectively, in the case of homogeneous nucleation.

A value of the exponent n of 3 was obtained for iPP, with a degree of crystalline transformation not higher than 20%, which in the case of homogeneous nucleation, represented two-dimensional growth with the generation of perfectly defined spherulitic structures with a linear growth rate, as observed from the analysis of the spherulitic growth rate in the same crystallization interval.

The analysis of the isothermal crystallization kinetics of nucleated iPP via the application of the Göler-Sachs treatment showed that in all cases, the value of the exponent n was 4, independent of the type of NA and the composition, as shown in Figure 2, where eq. (2) was applied for 0.05% of the NA Millad 3988.

Nagarajan et al.[21] recently described a value of $n = 3$ for iPP nucleated with 0.3% DBS for the isothermal crystallization between 115 and 132°C, compared with a value of $n = 2.5$ for pure iPP, which justified the existence of a change in the mode of sporadic nucleation in pure iPP to simultaneous in nucleated iPP, when a spherical crystallization geometry is assumed. The authors did not indicate the conditions of melt temperature and residence time before the isothermal crystallization and only pointed out that the residence temperature was higher than 198°C and that autonucleation phenomena in the PP could be ignored, although evidence for this was not confirmed.

In this work, the analysis of the crystallization kinetics was undertaken by the determination of the overall crystallization rate, with both stages of the crystallization process considered, that is, nucleation

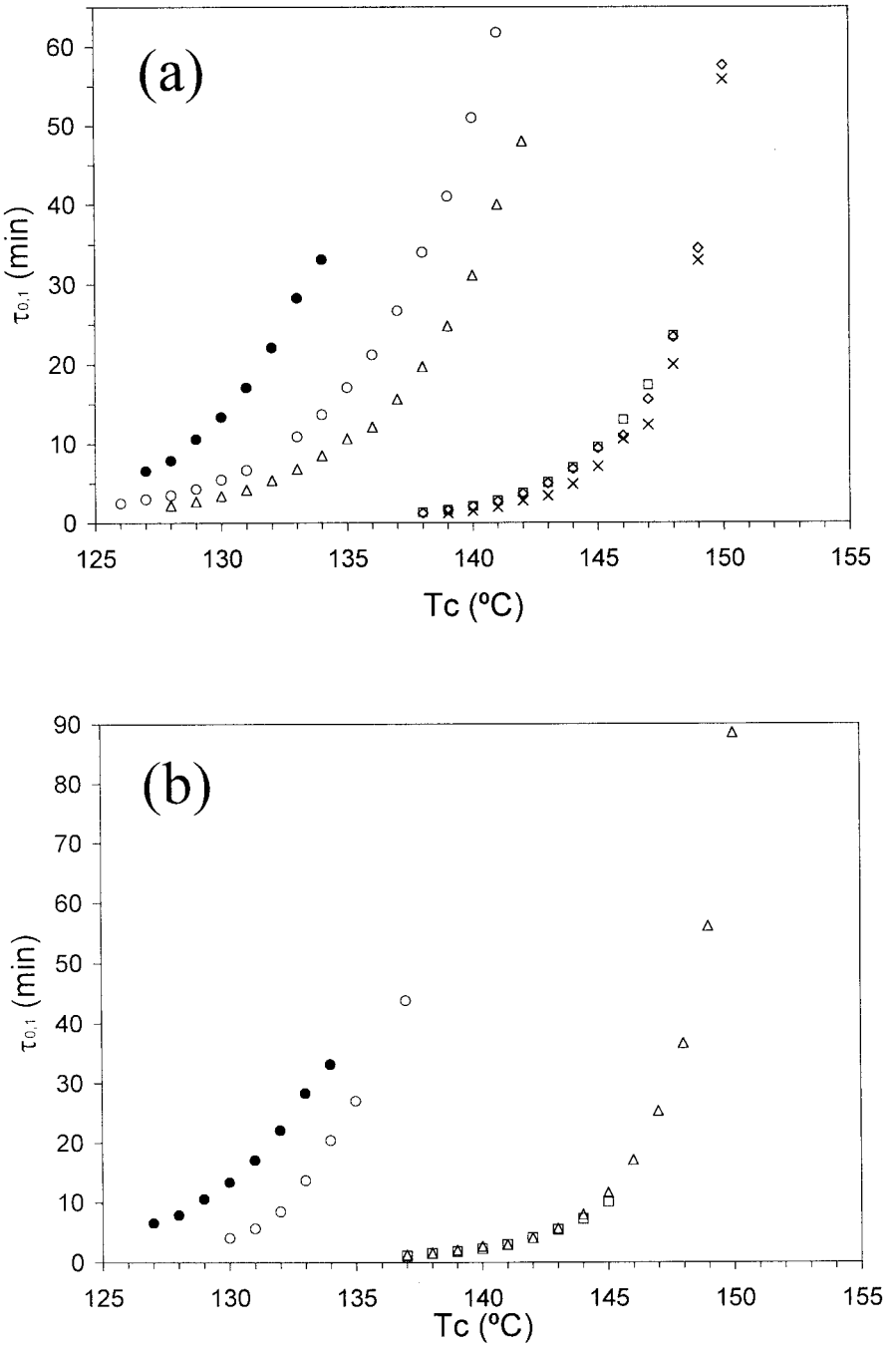

Figure 3 Evolution of $\tau_{0,1}$ with the temperature of crystallization for (●) iPP and NAs (a) Millad 3988 at the following concentrations: (○) 0.025%, (△) 0.05%, (□) 0.3%, (◇) 0.5%, and (×) 1% and (b) Geniset MD6001 at the following concentrations: (○) 0.1%, (△) 0.3%, and (□) 0.5%.

and growth. In this manner, the global rate (G) could be calculated as

$$G \approx \ln(\tau_i)^{-1} \tag{3}$$

over the timescale necessary for the crystallization of polymers, where G can be directly determined from the time necessary to reach a preestablished degree of crystalline transformation (i) denominated τ_i, and from its variation with the T_c, for a predetermined molecular weight.

The rate constant of the process (k) can be obtained from the following expression:[22]

$$k = \ln 2/(\tau_{0.5})^n \tag{4}$$

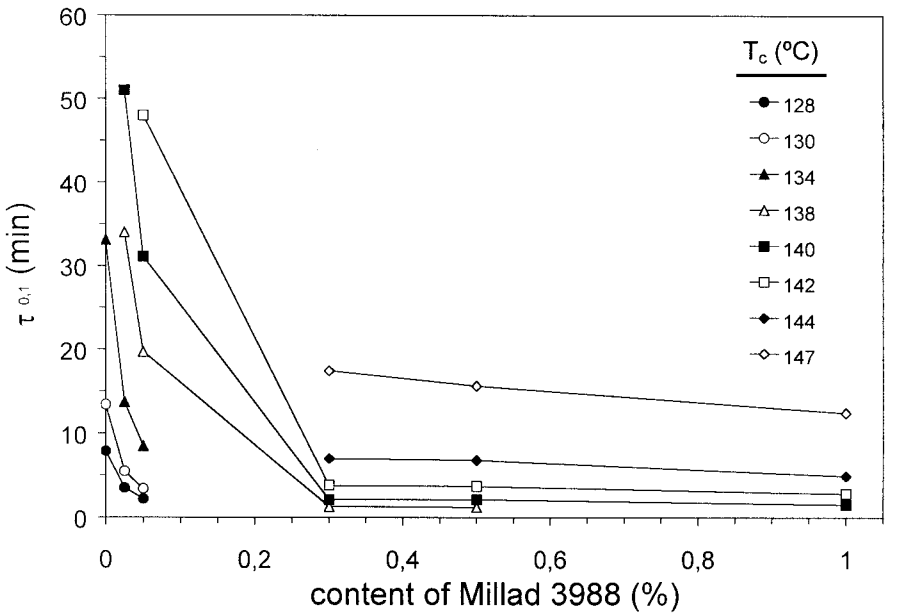

Figure 4 Evolution of $\tau_{0,1}$ with the concentration of NA Millad 3988 at the T_c's indicated.

where $\tau_{0.5}$ is the time necessary to reach 50% of crystalline transformation and the values of the exponent n are associated with each T_c.

G, compared with the values of the time necessary to reach 10% of crystalline transformation $\tau_{0.1}$ for each T_c, was a function of the concentration of the NA, as shown in Figure 3 for the NAs Millad 3988 and Geniset MDG001. Our first observation of relevance was the important increase in the range of T_c's in which iPP crystallized for a similar level of crystalline transformation, which led to a progressive reduction in this parameter, that is, an increase in the crystallization rate for each T_c as the concentration of the NA was increased. However, in both cases, the experimental results appeared to show a saturation of the nucleating effect for compositions of 0.3%, above which the rates appeared to level out. This saturation in the nucleating activity of sorbitol derivatives, demonstrated by the constant crystallization rate above a given concentration of NA, is clearly illustrated in Figure 4 for Millad 3988.

Because the crystallization rates observed for iPP as a function of the type and concentration of α-inducing

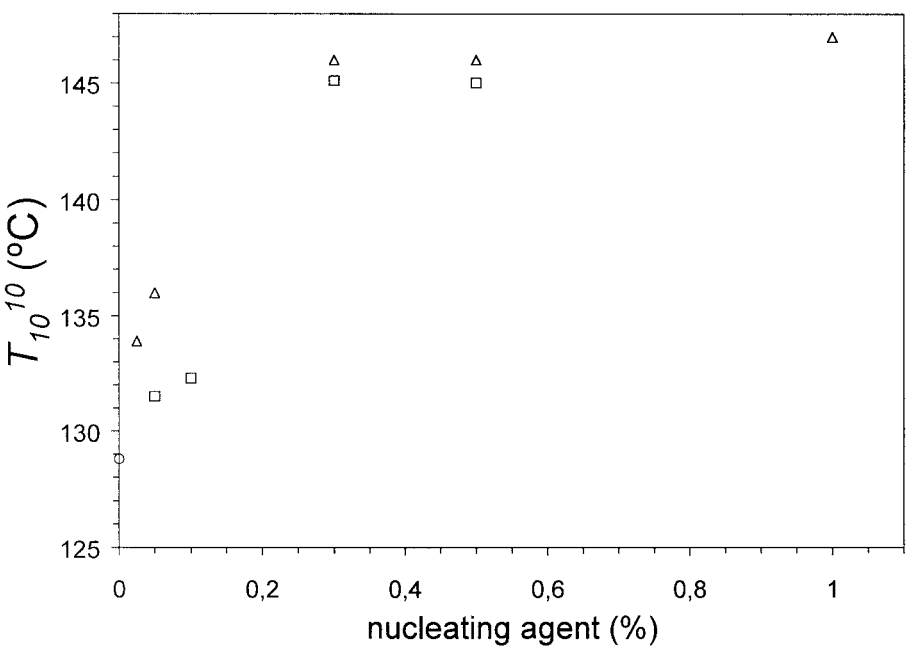

Figure 5 Variation of the parameter T_{10}^{10} as a function of composition for (○) iPP, (△) Millad 3988, and (□) Geniset MD6001.

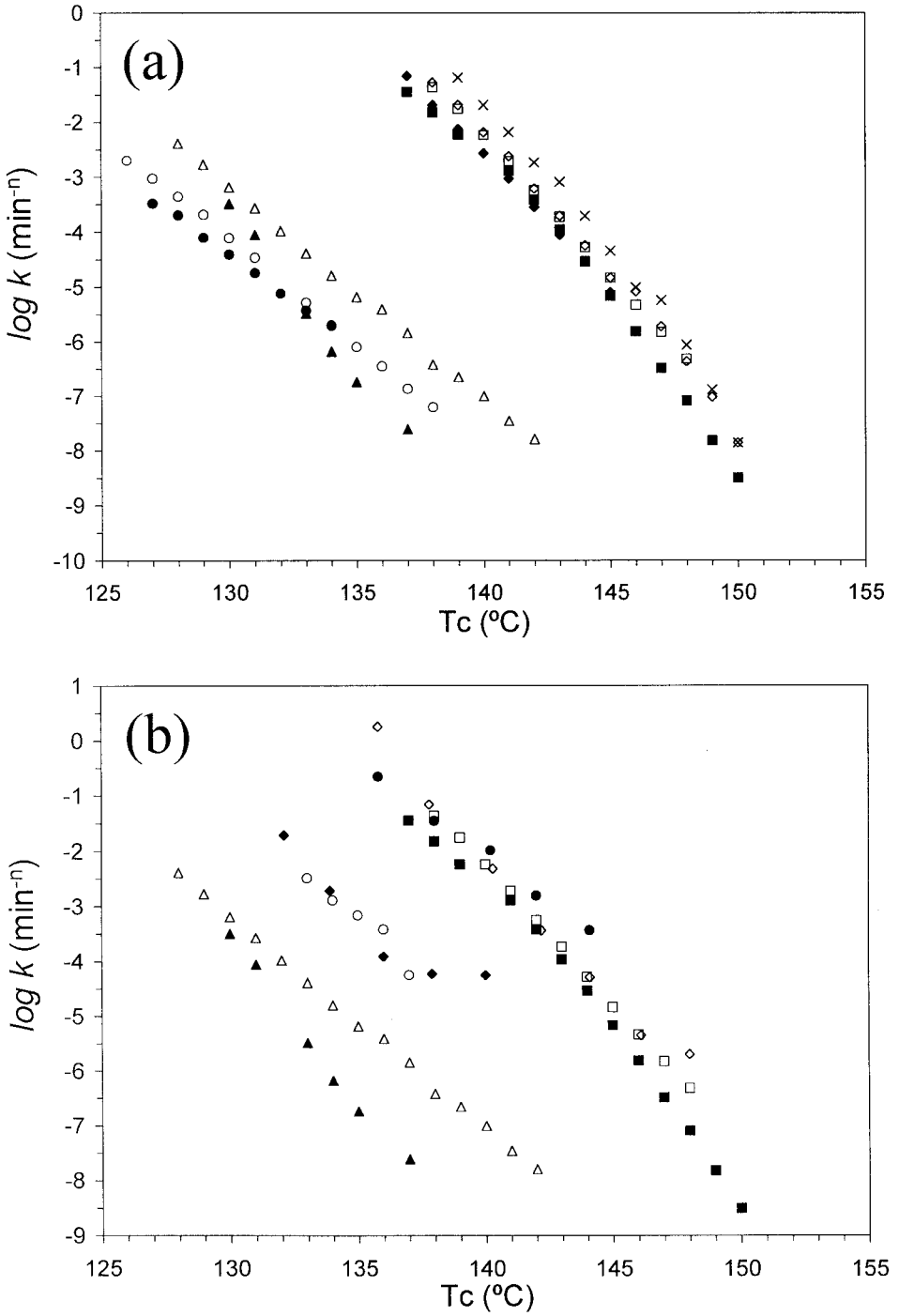

Figure 6 Variation in log k with T_c under isothermal conditions as a function of the type and concentration of NA: (a) comparison between (●) iPP, Millad 3988; (○) 0.025%, (△) 0.05%, (□) 0.3%, (◇) 0.5%, and (×) 1%; and Geniset MD6001 (▲) 0.1%, (■) 0.3%; and (◆) 0.5% and (b) Millad 3988 (△) 0.05% and (□) 0.3%; Geniset MD6001 (▲) 0.1% and (■) 0.3% with data from the literature (○) NC4 0.1%, (◆) DBS (EC1) 0.3%, (◇) EC4 0.3%, and (●) NC4 0.3%. See refs. 9 and 23.

NAs were significant, we aimed to establish in a rational manner the different nucleating efficiencies of each agent under isothermal crystallization conditions. However, a common T_c interval was not available, so to contrast the values, a parameter characteristic of rate and transformation was employed T_{10}^{10}, which represented the temperature of crystallization in isothermal conditions at which a crystalline transformation of 10% was reached in 10 min, obtained by interpolation shown in Figure 3(a, b).

Figure 5 represents the variation of the parameter T_{10}^{10} as a function of composition. As is evident from this figure, a higher value of this parameter, that is, a greater nucleating efficiency, was observed at compo-

TABLE I
Values of the Global Rate Constants k (min^{-n}), for Nucleated iPP at Different Concentrations of NA and T_c's

Temperature (°C)	NA and concentration			
	0.3%		0.5%	
	Millad 3988	Geniset MDG001	Millad 3988	Geniset MDG001
138	4.4×10^{-2}	1.5×10^{-2}	5.3×10^{-2}	2.1×10^{-2}
148	4.9×10^{-7}	8.3×10^{-8}	5.7×10^{-5}	2.9×10^{-5}

sitions of NA around 0.2% or lower, which produced a stabilization in the rate of crystalline conversion at higher compositions.

When a comparative analysis was made as a function of the global rate constants, k determined from eq. (4) [Fig. 6(a)], a number of significant points were observed. First, when we compared the rate constants observed for the same concentration of NA at different temperatures (Table I) in all cases k was higher for Millad 3988 than for its counterpart, Geniset MDG001. Second, a dramatic increase in k took place at around 0.3% NA for both NA's (Table II). Finally, although iPP presented a k of around 10^{-5} for a T_c of 131°C in the case of nucleated iPP, values of k of the same order could be obtained at a much higher T_c of 144–145°C for NA concentrations of 0.3% [Fig. 6(a)].

There is little kinetic data available in the case of sorbitol derivatives, and as shown as an example in Figure 6(b) our results for the behavior of the global rate constant as a function of the crystallization rate were compared with some values described in the literature[9,23] for three different sorbitol derivatives at concentrations of 0.1 and 0.3 wt%. The results described by Kim et al.[24] in the nucleation of iPP with *p*-Cl-*p*-methyldibenzylidine sorbitol (EC4) and bis(*p*-ethylbenzylidine sorbitol) (NC4) showed saturation effects in the nucleating activity at concentrations of 0.2–0.3% due to the fact that the number of effective nuclei was reduced at higher concentrations because of particle agglomeration.[25]

As shown in Table III, the influence of the composition of the sorbitol derivatives on the enthalpy associated with the isothermal crystallization (ΔH_c) process was very small, with a reduction in ΔH_c with increasing T_c, which allowed us to conclude that the nucleating action in this type of agent was very important with respect to the crystallization rate and not the level of crystallinity developed.

Melting behavior after isothermal crystallization

In Figure 7, the melting endotherms for pure iPP obtained by heating at 10°C min^{-1} after isothermal crystallization from the melt at the temperatures indicated are shown. This heating rate has been described as the most adequate for avoiding reordering and recrystallization processes during the heating cycle, which can have a decisive influence on the nature of the melting endotherm.[26] In all cases, the melting endotherms were very broad and began at temperatures very close to the T_c, presenting a broad and poorly defined shoulder at lower temperatures (T_m II) and a well-defined maximum at higher temperatures (T_m I) which both shifted to higher temperatures with increasing T_c.

There is a large body of published research on the melting behavior of iPP.[27–31] Excluding the presence of the trigonal (β) polymorphs,[32,33] the existence of multiple endotherms has been described as being due to various phenomena, such as the existence of recrystallization phenomena during the heating cycle after the isothermal process,[34,35] phase segregation and fractionation during crystallization,[36–38] or the existence of lamellar thickening due to the annealing process.[39–41] The existence of two monoclinic species associated with different crystalline morphologies, folded chain and extended chain, has also been suggested to explain the melting behavior,[42–45] although the formation from the melt at low undercooling of an extended chain morphology is highly improbable.[32] Other authors have attributed the double endotherm to the existence of melting–recrystallization–melting processes, excluding the possibility of the formation of two different species during isothermal crystallization,[46] although later it was shown that the monoclinic polymorph can exhibit different levels of disorder with respect to the up–down positioning of the

TABLE II
Values of the Global Rate Constants k (min^{-n}) for Nucleated iPP as a Function of Concentration

NA/T_c	NA concentration (%)				
	0.025	0.05	0.1	0.3	0.5
Geniset MDG001/137°C	—	—	2.5×10^{-8}	3.6×10^{-2}	7.1×10^{-2}
Millad 3988/138°C	6.4×10^{-8}	3.9×10^{-7}	—	4.4×10^{-2}	5.3×10^{-2}

TABLE III
Values of ΔH_c (Jg^{-1}) as a Function of the T_c and the Type and Concentration of NA

		iPP/Millad 3988					iPP/Geniset MDG001		
T_c (°C)	iPP	0.025%	0.05%	0.3%	0.5%	1%	0.1%	0.3%	0.5%
126	—	92.9	—	—	—	—	—	—	—
127	87.4	93.8	—	—	—	—	—	—	—
128	87.6	93.5	92.8	—	—	—	—	—	—
129	88.1	92.5	93.6	—	—	—	—	—	—
130	87.4	92.7	93.1	—	—	—	93.9	—	—
131	86.9	91.9	92.9	—	—	—	94.0	—	—
132	85.9	—	93.7	—	—	—	93.2	—	—
133	86.4	92.6	92.8	—	—	—	93.4	—	—
134	85.3	93.0	92.5	—	—	—	92.7	—	—
135	—	92.3	91.8	—	—	—	93.6	—	—
136	—	91.6	91.6	—	—	—	—	—	—
137	—	91.4	90.9	—	—	—	92.7	96.8	94.5
138	—	90.7	91.5	93.9	93.8	—	—	95.8	95.2
139	—	90.0	92.3	94.9	94.2	92.7	—	96.5	94.2
140	—	91.2	90.5	94.3	92.9	93.3	—	—	95.6
141	—	90.5	89.6	95.3	93.5	92.7	—	94.9	95.6
142	—	—	90.3	94.2	92.6	91.5	—	95.1	95.2
143	—	—	—	93.8	93.7	92.4	—	94.0	94.2
144	—	—	—	94.2	93.5	91.6	—	94.3	93.6
145	—	—	—	93.6	92.7	92.7	—	92.9	92.4
146	—	—	—	94.1	94.6	91.4	—	92.3	
147	—	—	—	92.8	93.3	92.3	—	91.0	
148	—	—	—	93.1	93.8	92.4	—	91.4	
149				—	92.9	91.4	—	90.8	
150				—	91.7	90.8	—	90.4	

polypropylene chains to such an extent that the double endotherm may be considered a result of the melting of a monoclinic structure with a certain degree of order and a crystallographic symmetry $P2_1/c$, and another with a certain level of disorder, with crystallographic symmetry $C2/c$, denominated α_2 and α_1, respectively.[47,48]

Other authors have suggested that the crystals that melt at higher temperatures originate during the process of primary crystallization, whereas the crystals that grow in the interfibrillar regions during the secondary crystallization process melt at lower temperatures.[49] Recently, the melting of tangential, or cross-hatched, lamellae has been proposed for the endothermic behavior at lower temperatures the higher temperature peak being associated with the melting of radial lamellae and reorganized tangential lamellae.[50] Very recently, Zhu et al.,[51] in isothermal crystallization studies with DSC and wide- and small-angle X-ray diffraction, suggested that in the interval of $T_c < 117$°C, the lamellae formed are imperfect and can undergo melting–recrystallization–melting processes during the heating process, which lead to the formation of double endotherms. On the contrary, for $T_c > 136$°C, two families of lamellae were formed, which directly generated the melting behavior observed. At intermediate T_c's, the authors justified the formation of a unique family of lamellae with a relatively narrow thickness distribution, which gave rise to a unique melting peak.

The crystallization interval for iPP used in this work was 127–133°C, and evidently, as shown in Figure 7, the heterogeneity in the melting endotherms did not appear to confirm the formation of a unique family of lamellae with a narrow thickness distribution, thus disagreeing with the suggestion of Zhu et al.[51] On the contrary, fundamentally due to the shift to higher temperatures observed for both the T_mII and the well-defined maximum, T_mI with increasing T_c, it seems more reasonable to associate the melting behavior to the existence of melting–recrystallization–melting phenomena. In other words, the broad shoulder observed at lower temperatures corresponded with the crystals generated under isothermal conditions and shifted to higher temperatures with T_c, that is, whereas still being imperfect crystals, their degree of imperfection was progressively less because T_mII increased. When recrystallization took place, even at a heating rate of 10°C min^{-1}, the crystals that were then generated were formed at higher T_c's, and consequently, T_mI also progressively increased. If the family of crystals that gave rise to T_mI were formed exclusively due to crystalline segregation during the isothermal crystallization process, the crystallites formed from the recrystallization phenomenon after the melting of the family associated with T_mII would give rise

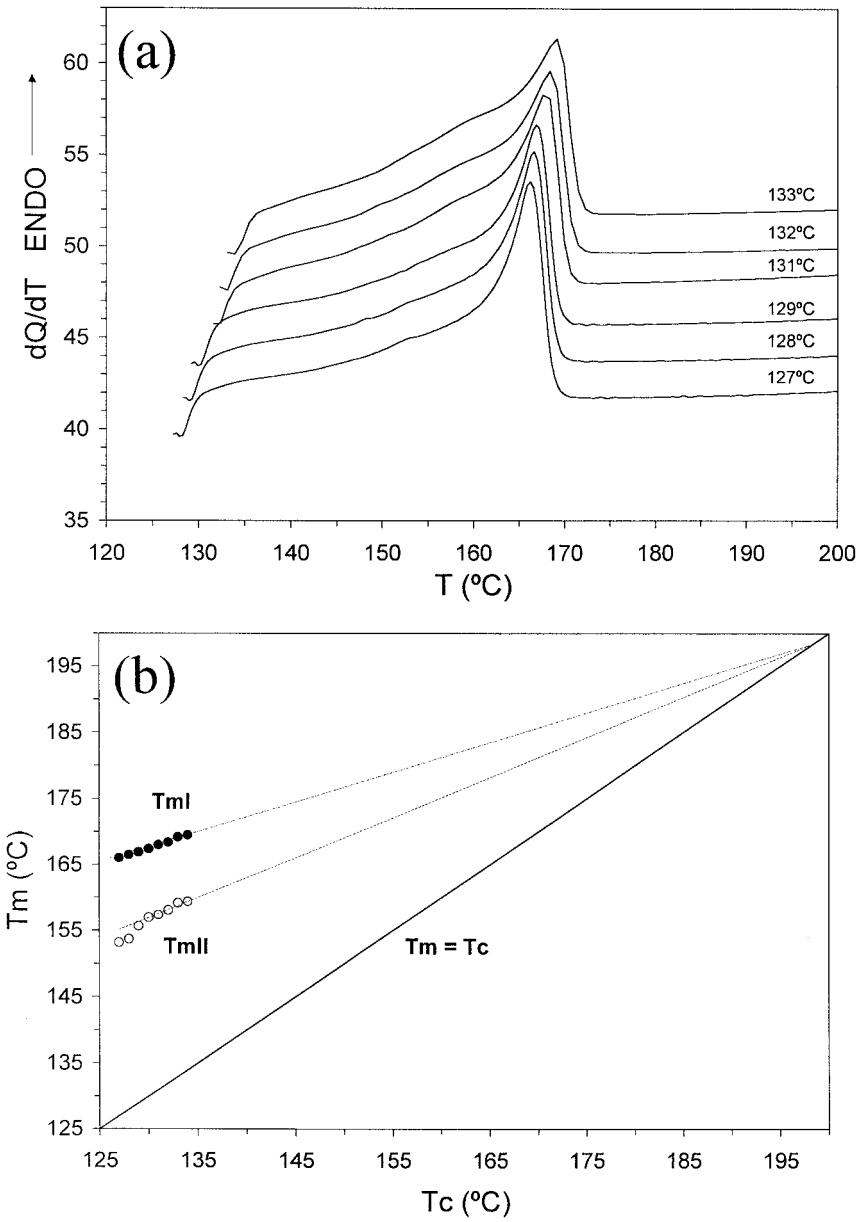

Figure 7 (a) Melting thermograms for pure iPP recorded at a heating rate of 10°C min^{-1} after isothermal crystallization at the temperatures indicated and (b) the corresponding variation in the T_m's T_mI and T_mII as a function of the T_c.

to a third melting peak, above that of T_mI because they would have been developed at a higher T_c.

One of the most used extrapolation methods[52–57] for the determination of the T_m in conditions of thermodynamic equilibrium is based on the implicit relationship between the crystal size and the T_m proposed by Gibbs[58] and Thomson:[59]

$$T_m = T_m^0[1 - (2\sigma_{ec}/\xi\,\Delta H_m)] \quad (5)$$

where T_m^0 is the equilibrium melting temperature, σ_{ec} is the interfacial free energy associated with the basal face of the crystallite and ξ is the crystal size. In this expression, it is assumed that the lateral dimensions of the lamellar crystallite are much greater than its thickness and do not depend on the nature of the interfacial structure.[60] At low levels of crystallinity, the size of the crystallite can be considered to be practically identical to the critical nucleus size, and by the establishment of a specific crystalline nucleation process where the free energy of melting is independent of the level of crystallinity, one can consider the relation between T_m and T_c given by the following expression:[61]

$$T_m = T_m^0[1 - (\beta/2m)] + (\beta/2m)T_c \quad (6)$$

where $\beta = \sigma_{ec}/\sigma_{en}$ and $m = \xi/\xi'$; σ_{ec} and σ_{en} are the basal interfacial free energies of the mature crystallite

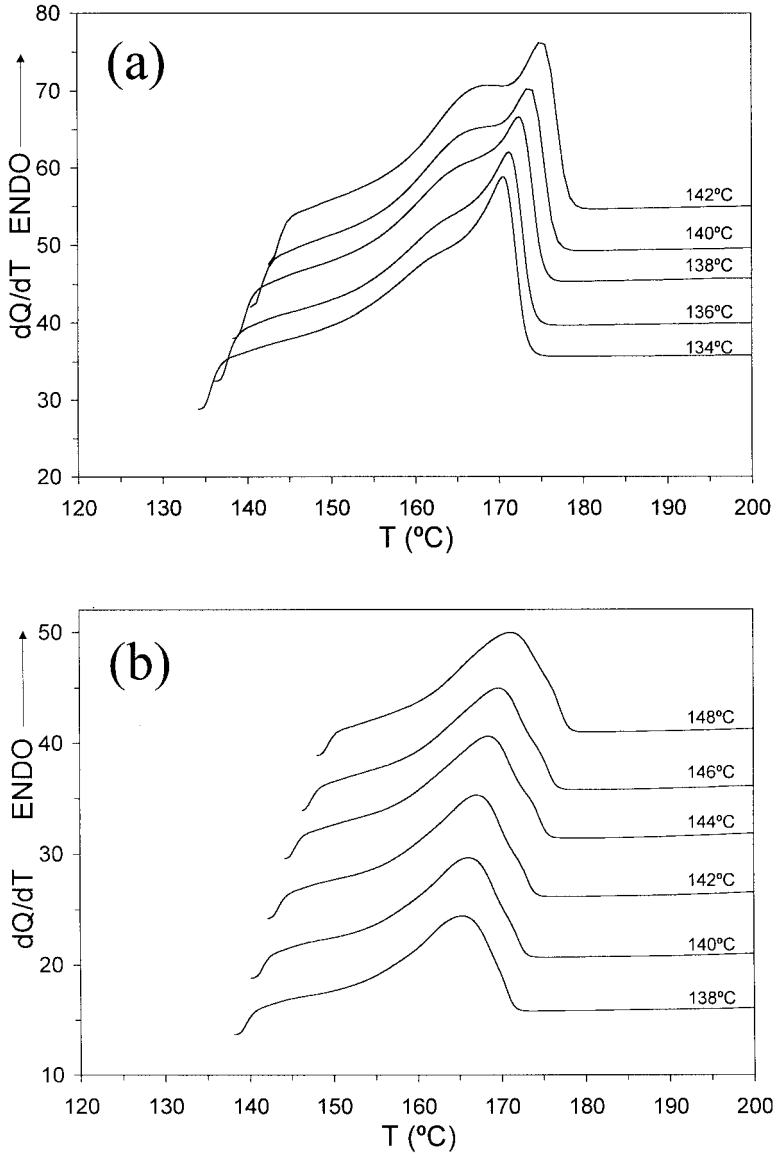

Figure 8 Melting thermograms for iPP/Millad 3988 at concentrations of (a) 0.05 % and (b) 0.5%, recorded at a heating rate of 10°C min^{-1} after isothermal crystallization at the temperatures indicated.

and the nucleus, respectively; and ξ and ξ' are the size of the crystal and the size of the critical nucleus. For values of $\beta = 1$ and $m = 1$, an extrapolation can be made to the straight line $T_m = T_c$ with a slope of 0.5 because the previous expression becomes

$$T_m = (1/2)(T_m^0 + T_c) \quad (7)$$

The representation of the apparent T_m corresponding to a crystal developed at a particular T_c, for low levels of crystallinity, can be interpreted in terms of the type of nucleation involved and of the relationship that exists between the dimensions of the crystallite that melts and the dimensions of the crystalline nucleus from which it was developed.

The representation of the values of both T_mI and T_mII showed a linear variation with the T_c [Fig. 7(b)] with slopes of 0.45 and 0.65, respectively. These values were very close to the theoretical value of 0.5, although the larger slope of 0.65 associated with the behavior of the lower temperature shoulder seemed to show the influence of heating on the family of more imperfect and/or smaller crystals, without doubt through the crystalline reorganization process previously mentioned,[62] although a process of lamellar thickening through annealing in polypropylene is more difficult when there is a higher number of defects in the stereoregularity and/or a greater the molecular weight.[49]

The extrapolation of both variations to the line corresponding with $T_m = T_c$ led to a value of 198°C in both cases, which could be considered the T_m^0 for this system.

Many values have been reported in the literature for the T_m^0 of polypropylene, and these vary between 174

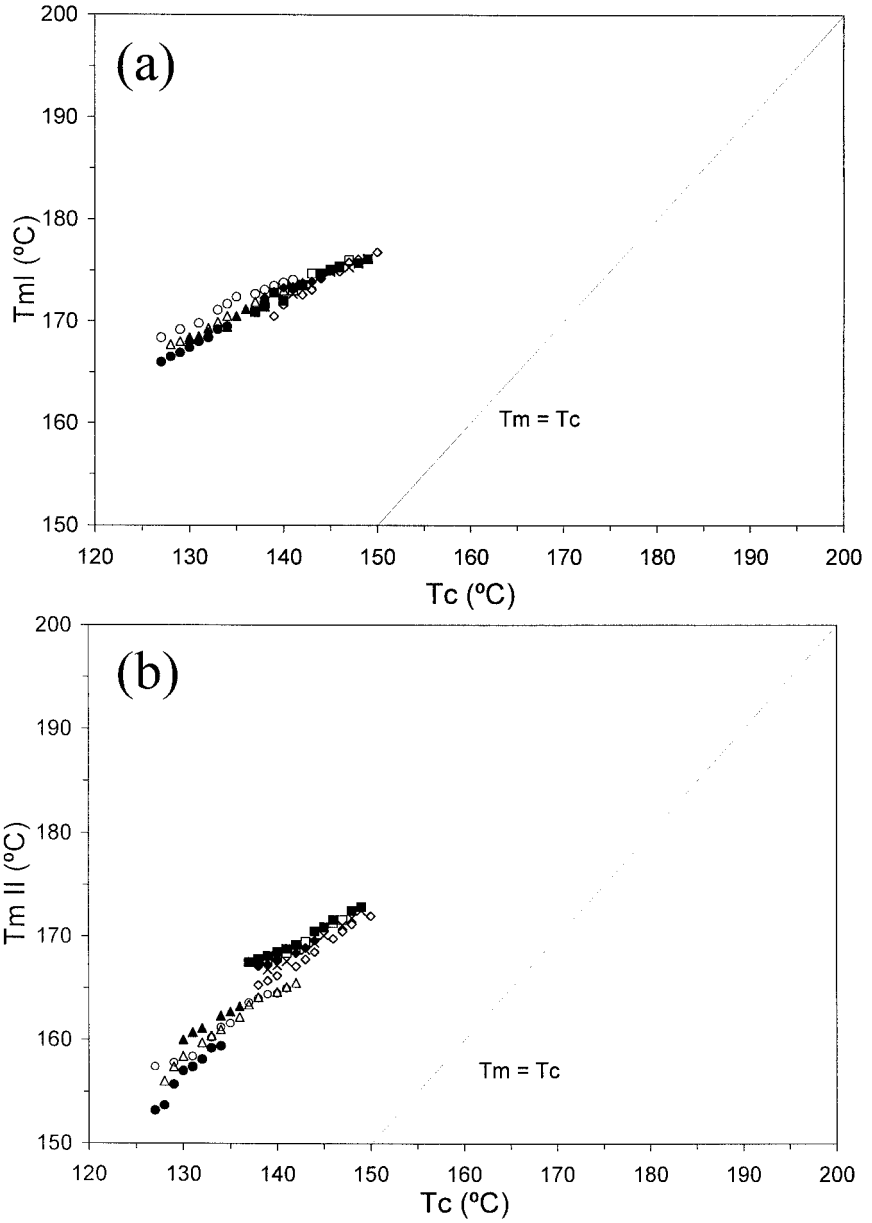

Figure 9 Variation of T_m's (a) T_mI and (b) T_mII for all the monoclinic series with T_c after crystallization under isothermal conditions; (●) iPP; Millad 3988 (○) 0.025%, (△) 0.05%, (□) 0.3%, (◇) 0.5%, and (×) 1%; and Geniset MD6001 (▲) 0.1%, (■) 0.3%, and (◆) 0.5%.

and 220°C,[63–65] the origin of this large range being due to differences in molecular weight, microstructure, and thermal history. Although it is not the objective of this article to enter into a detailed discussion in this regard, it is convenient to point out some relevant features here. It is well known that one of the most important factors among those that affect the value of T_m^0 in iPP is the stereoregularity, although widely differing values have been described. Thus, for a sample of PP with 95.8% of isotactic pentads, an extrapolated value of T_m^0 = 185°C has been reported,[49] whereas for another sample with 95% isotactic triads a value of 207°C was given, although the real extrapolation did not give values higher than 197°C.[62] Factors such as the thermal history of the melt, crystallization interval, and heating rate, along with the molecular weight and molecular weight distribution, can condition and justify the existence of such large discrepancies.[66]

The melting behavior after isothermal crystallization of iPP depended on the type of NA and its composition. In the case of the agents Millad 3988 and Geniset, the phenomenon of double endotherms was also present, which was more noticeable at lower the concentrations of NA and higher T_c's, as shown in Figure 8.

As previously mentioned, the isothermal crystallization of iPP in the presence of NAs that induced the

monoclinic polymorph used in this study, occurred in the majority of cases at crystallization temperatures above 136°C. Zhu et al.[51] recently showed that a sample crystallized above 136°C presented a bimodal distribution in their small-angle X-ray scattering diagrams, indicating the existence of two lamellar families of different thickness. In agreement with the results obtained by Norton and Keller,[67] the family of greater thickness corresponded to radial lamellae, which grew more quickly at higher temperatures[68] than the thinner tangential lamellae. It has also been reported that the birefringence of the monoclinic spherulites increases with temperature during the heating process, until the high temperature endotherm is reached, which supports the idea of melting of the tangential lamellae before that of the radial lamellae.[69] In our case, the crystallization rate of iPP in the presence of 0.5% Millad 3988 is much higher than that for 0.05% NA, resulting in a much larger population of radial lamellae. Thus, the effect on the appearance of the double endotherms is much more important in the case of the lower NA concentration, where the population of the tangential lamellae is larger.

When the data corresponding to the relation T_m versus T_c for the whole series were collated, it was confirmed that in the case of T_mI, the extrapolation of this family of results with very little dispersion led to a global value of T_m^0 = 198°C, with a slope almost equal to 0.46, Figure 9(a), and showed no evidence for any influence of the type of NA or the composition, except that of the expected increase in the T_m with the T_c. In the case of T_mII [Fig. 9(b)], the relation T_m versus T_c also seemed to be unaffected by the nature of the NA, but was influenced by the composition at low concentrations of agent, which was especially notable for Millad 3988. The corresponding global extrapolation also led to values of T_m^0 of approximately 198°C but with a variation in the gradient between 0.65 and 0.5. These results are in agreement with those of Chen and Xu,[70] which point toward the influence of the NA on the crystallization rate but not on the T_m in thermodynamic equilibrium.

CONCLUSIONS

The crystallization kinetics of iPP and two α-nucleated iPP systems based on sorbitol derivatives were analyzed in isothermal conditions as a function of the concentration of NA. As one might expect, the incorporation of these agents led to an important increase in the isothermal T_c of iPP, along with a reduction in the crystallization interval and an increase in the crystallization rate with increasing NA content. Comparable values of the global rate constant for iPP were achieved at significantly higher temperatures with these nucleated systems. The dramatic increase in all the kinetic parameters observed in the nucleated materials occurred at around 0.3% NA, above which the effect saturated. With respect to melting, the appearance of double endotherms in the nucleated systems was analogous to the case for iPP and seemed to originate from melting–recrystallization–melting phenomena. No difference was observed in the T_m^0 between iPP and the nucleated systems.

The authors thank M. A. López Galán at the Instituto de Ciencia y Tecnología de Polímeros for her collaboration.

References

1. Turnbull, D; Fischer, J. C. J. Chem Phys 1949, 17, 71.
2. Mandelkern, L. In Crystallization of Polymers; McGraw-Hill: New York, 1964.
3. Lauritzen, J. I.; Hoffman, J. D. J Res Natl Bur Stand A 1960, 64, 73.
4. Hoffman, J. D.; Davis, G. T.; Lauritzen, J. I. In Treatise on Solid State Chemistry; Hannay B., (Ed.); Plenum: New York, 1976; Vol. 3.
5. Thierry, A.; Straupé, C.; Lotz, B.; Wittmann, J. C. Polym Commun 1990, 31, 299.
6. Quan, Z.; Yongxi, S.; Hongpeng, W. J Polym Mater 1992, 9, 59.
7. Thierry, B.; Fillon, C.; Strampi, B.; Lotz, A.; Wittmann, J. C. Prog Colloid Polym Sci 1992, 87, 28.
8. Fillon, B.; Lotz, B., Thierry, A.; Wittmann, J. C. J Polym Sci Part B: Polym Phys 1993, 31, 1395.
9. Kim, C. Y.; Kim, Y. C.; Kim, S. C. Polym Eng Sci 1993, 33, 1445.
10. Shephard, T. A.; Delsorbo, C. R.; Louth, R. M.; Walborn, J. L.; Norman, D. A.; Harvey, N. G.; Spontak, R. J. J Polym Sci Part B: Polym Phys 1997, 35, 2617.
11. Bauer, T.; Thomann, R.; Mülhaupt, R. Macromolecules 1998, 31, 7651.
12. Millner, O.; Titus, G. Chem Des Automation News 1990, 5, 10.
13. Smith, T. L.; Masilamani, D.; Bui, L. K.; Brambilla, R.; Khanna, Y. P.; Gabriel, A. J Appl Polym Sci 1999, 52, 591.
14. Smith, T. L.; Masilamani, D.; Bui, L. K.; Khanna, Y. P.; Bray, R. G.; Hammond, W. B.; Curran, S.; Belles, J. J.; Binder-Castelli, S. Macromolecules 1994, 27, 3147.
15. Anonymous., Plast Addit Compd 2000, 3(3), 30.
16. Marco, C.; Ellis, G.; Gómez, M. A.; Arribas, J. M. J Appl Polym Sci 2002, 84, 2440.
17. Marco, C.; Gómez, M. A.; Ellis, G.; Arribas, J. M. J Appl Polym Sci, 2002, 84, 1669.
18. Ziabicki, A.; Alfonso, G. C. Colloid Polym Sci 1994, 272, 1027.
19. Alfonso, G. C.; Ziabicki, A. Colloid Polym Sci 1995, 273, 317.
20. Van Göler, F.; Sachs, G. Z Phys 1932, 77, 281.
21. Nagarajan, K.; Levon, K.; Myerson, A. S. J Therm Anal Cal 2000, 59, 497.
22. Kim, S. P.; Kim, S. C. Polym Eng Sci 1991, 31, 110.
23. Wang, K.; Mai, K.; Zeng, H. J Appl Polym Sci 2000, 78, 2547.
24. Kim, Y. C.; Kim, C. Y.; Kim, S. C. Polym Eng Sci 1991, 31, 1009.
25. Mitra, D.; Misra, A. J Appl Polym Sci 1988, 36, 387.
26. Wlochowicz, A.; Eder, M. Polymer 1984, 25, 1268.
27. Fujiwara, Y. Colloid Polym Sci 1975, 253, 273.
28. Lovinger, A. J.; Chua, J. O.; Gryte, C. C. J Polym Sci Polym Phys Ed 1977, 15, 641.
29. Varga, J. J Thermal Anal 1989, 35, 1891.
30. Cheng, S. Z. D.; Janimag, J. J.; Zhang, A.; Hsieh, E. T. Polymer 1991, 32, 648.
31. Paukkeri, R.; Lehtinen, A. Polymer 1993, 34, 4075.
32. Samuels, R. J. J Polym Sci Polym Phys Ed 1975, 13, 1417.
33. Lotz, B.; Whitmann, J. C.; Lovinger, A. J. Polymer 1999, 37, 4979.
34. Yadav, Y. S.; Jain, P. C. Polymer 1986, 27, 721.

35. Passingham, C.; Hendra, P. J.; Cudby, M. E. A.; Zichy, V.; Weller, M.; Eur Polym J 1990, 26, 631.
36. Kawai, T. Makromol Chem 1965, 84, 290.
37. Cox, W. W.; Duswalt, A. A. Polym Eng Sci 1967, 7, 631.
38. Kawai, T. Kollid Z Z Polym 1969, 229, 116.
39. Hoffman, J. D.; Weeks, J. J. J Chem Phys 1965, 42, 4301.
40. Kamide, K.; Kamaguchi, K. Makromol Chem 1972, 162, 219.
41. Mezghani, K.; Campbell, R. A.; Phillips, P. J. Macromolecules 1994, 27, 997.
42. Pae, K. D.; Sauer, J. A. J Appl Polym Sci 1968, 12, 1901.
43. Sieglaff, C. L.; O'Leary, K. J Polym Prepr 1969, 10, 57.
44. Clough, S. B. J Macromol Sci Phys 1970, 4, 199.
45. Luch, D.; Yeh, G. S. Y. J Polym Sci Polym Phys Ed 1973, 11, 467.
46. Petraccone, V.; Rosa, C. D.; Guerra, G.; Tuzi, A. Makromol Chem Rapid Commun 1984, 5, 631.
47. Corradini, P.; Napolitano, R.; Oliva, L.; Petraccone, V.; Pirozzi, B. Makromol Chem Rapid Commun 1982, 3, 753.
48. Guerra, G.; Petraccone, V.; Corradini, P.; Rosa, C. D.; Napolitano, R.; Pirozzi, B.; Giunchi, G. J Polym Sci Polym Phys Ed 1984, 22, 1029.
49. Martuscelli, E.; Pracella, M.; Crispino, L. Polymer 1983, 24, 693.
50. Al-Raheil, I. A.; Qudah, A. M.; Al-Share, M. J Appl Polym Sci 1998, 67, 1267.
51. Zhu, X.; Yan, D.; Tan, S.; Wang, T.; Yan, D.; Zhou, E. J Appl Polym Sci 2000, 77, 163.
52. Marco Rocha, C.; Bello Antón, A.; Gómez Fatou, J. M. Makromol Chem 1978, 179, 1333.
53. Marco Rocha, C.; Gómez Fatou, J. M.; Bello Antón, A.; Blanco Magadán, A. Makromol Chem 1980, 181, 1357.
54. Bello Antón, A.; Lazcano Ureña, S.; Marco Rocha, C.; Gómez Fatou, J. M. J Polym Sci Polym Chem Ed 1984, 22, 1197.
55. Sánchez, A.; Marco, C.; Fatou, J. G.; Bello, A. Makromol Chem 1987, 188, 1205.
56. Cimmino, S.; DiPace, E.; Martuscelli, E.; Silvestre, C. Polymer 1991, 32, 1080.
57. Rodríguez-Arnold, J.; Zhang, A.; Cheng, S. Z. D.; Lovinger, A.; Hsieh, E. T.; Chu, P.; Johnson, T. W.; Honnell, K. G.; Geerts, R. G.; Palackal, S. J.; Hawley, G. R.; Welch, M. B. Polymer 1994, 35, 1884.
58. Gibbs, J. W. The Scientific Work of J. Willard Gibbs; Longmans Green: New York, 1908; Vol. I.
59. Thomson, J. J. Applications of Dynamics; Macmillan: London, 1988.
60. Mandelkern, L. J Polym Sci 1960, 47, 494.
61. Alamo, R. G.; Viers, B. D.; Mandelkern, L. Macromolecules 1995, 28, 3205.
62. Hbhadon, A. O. J Appl Polym Sci 1992, 46, 2123.
63. Wunderlich, B. Macromolecular Physics; Crystal Melting, Vol. III: Academic: New York, 1980.
64. Fatou, J. G. In Handbook of Polyolefins: Vasile, C.; Seymour, R. B.; Eds.; Marcel Dekker: New York, 1993.
65. Varga, J. In Polypropylene: Structure, Blends and Composites; Karger-Kocsis, J. Ed.; Structure and Morphology, Vol. I: Chapman & Hall: London, 1995.
66. Martuscelli, E.; Avella, M.; Segre, A. L.; Rossi, E.; Di Drusco, G.; Galli, P.; Simonazzi, Y. Polymer 1985, 26, 259.
67. Norton, D. R.; Keller, A. Polymer 1985, 26, 704.
68. Janimak, J. J.; Cheng, S. Z. D.; Giusti, P. A.; Hiseh, E. T. Macromolecules 1991, 24, 2253.
69. Mezghani, K.; Camphell, R. A.; Phillips, P. J. Macromolecules 1994, 27, 997.
70. Chen, Y.; Xu, M. Gaofenzi Xuebao 1998, 2, 240.